Supplemental Figure legends

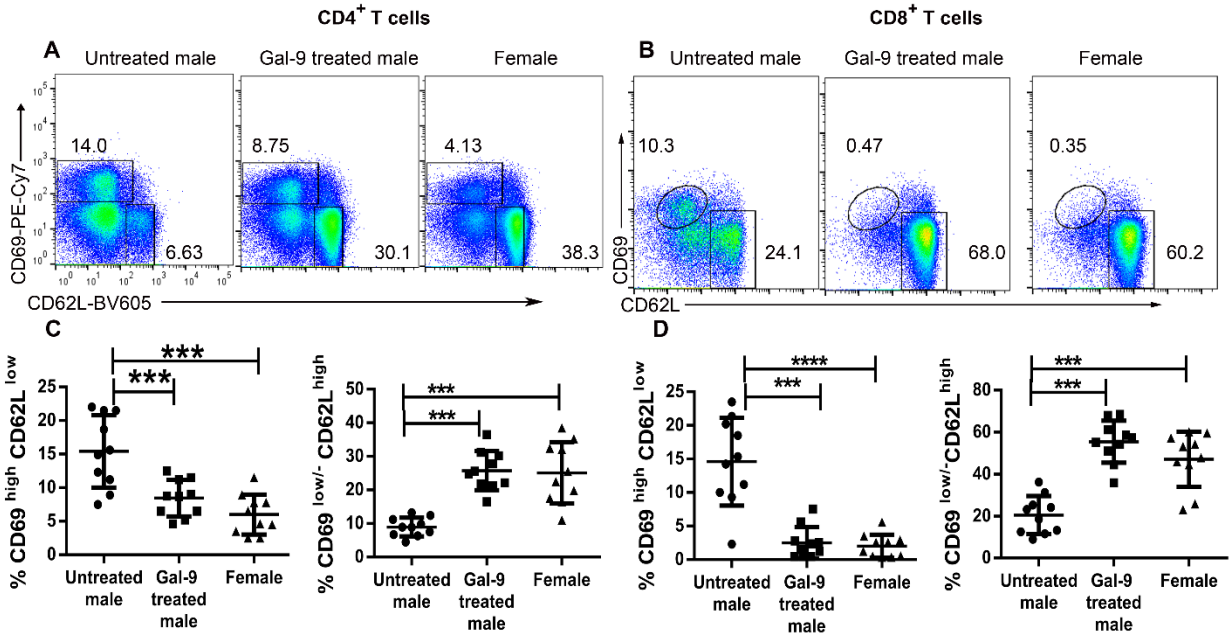

Supplemental Figure 1. Administration of Gal-9 inhibits CD69 expression on T cells.

Representative flow cytometric figures of expression of CD69 and CD62L on $CD4^+$ T cells (**A**) and $CD8^+$ T cells (**B**). Frequency of $CD69^{high}/CD62L^{low}$ and $CD69^{low/-}/CD\ 62L^{high}$ cells on $CD4^+$ T cells (**C**) and $CD8^+$ T cells (**D**) were analyzed by flow cytometry. Data points represent individual mice (N=10). Data are representative of two independent experiments. Mean±SD. One way ANOVA with Dunnett's multiple comparison was used to test the statistical significance. P value denoted as *<0.05, **<0.01 and ***< 0.001 versus control.

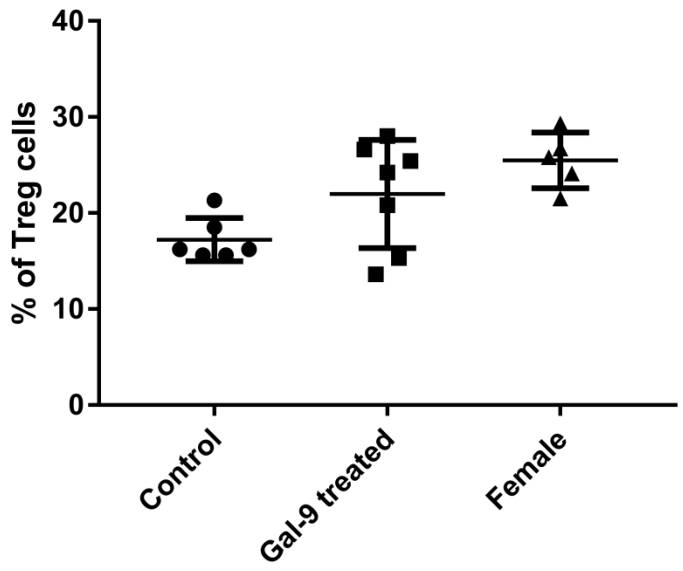

Supplemental Figure 2. Treg profile of BXSB/MpJ mice remain unchanged upon Gal-9 treatment.

Splenocytes from male BXSB/MpJ mice with and without Gal-9 treatment and female littermates were analyzed. % of $CD4^+$ $Foxp3^+$ T cells was plotted. Each dot presents individual mice.

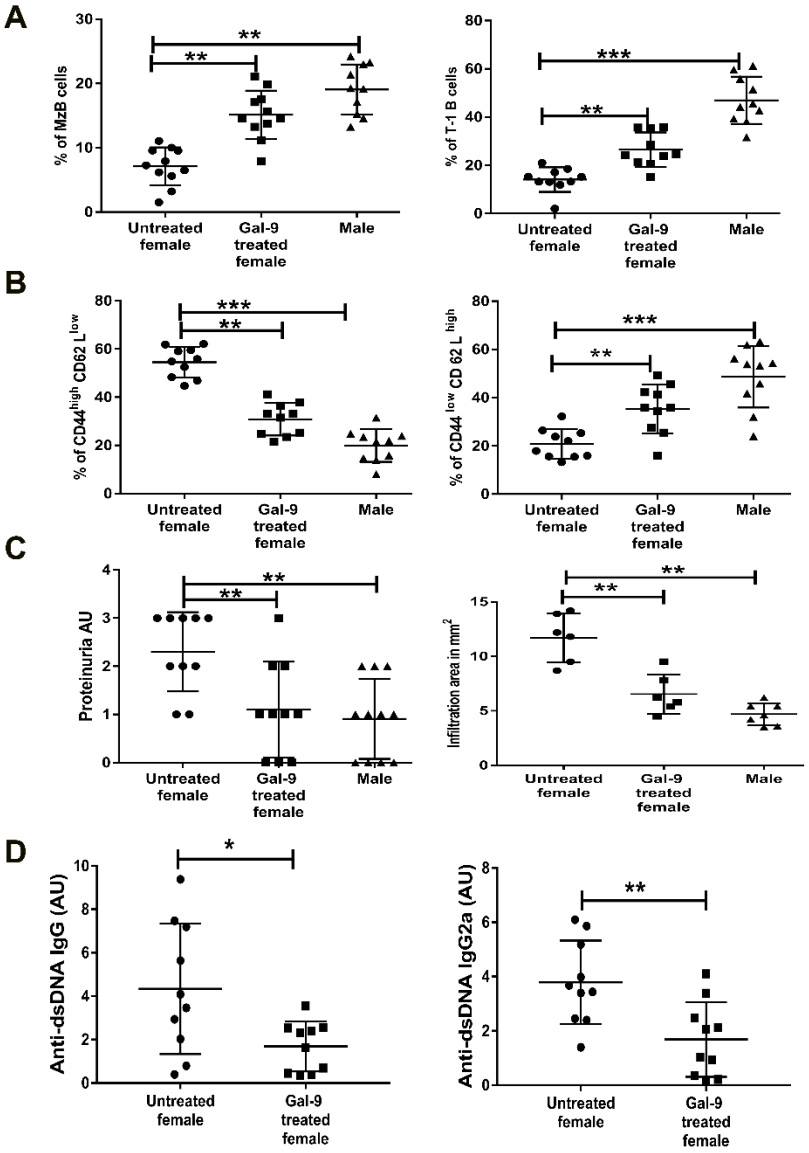

Supplemental Figure 3. Gal-9 administration reduces lupus pathogenesis in NZB/W F1 mice.

Splenocytes from Gal-9 treated female, untreated female and age-matched male littermates of NZB/W F1 mice were analyzed for expression of different markers on $CD19^+$ B cells and $CD3^+$ T cells. Frequency of MzB cells and T1B cells (**A**) CD44 ^{high} CD62 ^{low} and CD44 ^{low} CD62L ^{high} (**B**) of Gal-9 treated female along with age matched untreated female and male littermates. Mean

± SD of 10 mice in each group are shown. (**C**) Proteinuria levels and glomeruli size of 32-week-old both Gal-9 treated and untreated control female along with male littermates. Mean ± SD. Each dot represents individual mice (**D**) Serum levels of anti-ds-DNA IgG and IgG2a in Gal-9 treated and untreated control female mice. Mean ± SD of 10 mice in each group are shown. One way ANOVA with Dunnett's multiple comparison was used to test the statistical significance for data presented in Figure A, B and Kruskal Wallis testing was performed followed by Dunn's test for Figure C. Mann-Whitney test with Welch's correction was used for data represented in Figure D. P value denoted as *<0.05, **<0.01 and ***< 0.001.

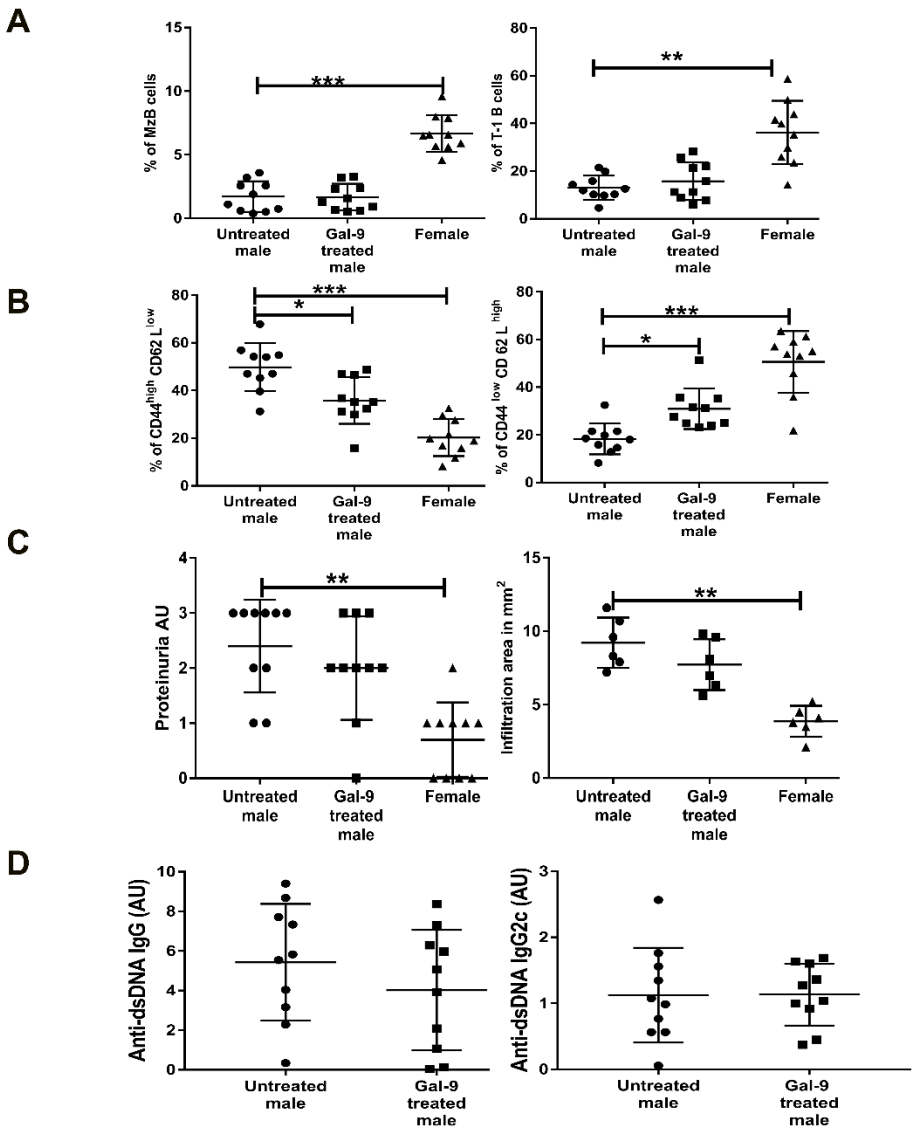

Supplemental Figure 4. Gal-9 unable to reduce lupus pathogenesis when treatment started after onset of the disease.

Splenocytes from Gal-9 treated male, untreated male and age-matched female littermates of BXSB/MpJ mice were analyzed for expression of different markers on $CD19^+$ B cells and $CD3^+$ T cells. Frequency of MzB cells and T1B cells (A) CD44 ^{high} CD62 ^{low} and CD44 ^{low} CD62L ^{high} (B) of Gal-9 treated male along with age matched untreated male and female littermates. Mean $\pm$

SD of 10 mice in each group are shown. (**C**) Proteinuria levels and glomeruli size of 19-week-old both Gal-9 treated and untreated control male along with female littermates. Mean ± SD. Each dot represents individual mice (**D**) Serum levels of anti-ds-DNA IgG and IgG2c in Gal-9 treated and untreated control male mice. Mean ± SD of 10 mice in each group are shown. One way ANOVA with Dunnett's multiple comparison was used to test the statistical significance for data presented in Figure A, B and Kruskal Wallis testing was performed followed by Dunn's test for Figure C. Mann-Whitney test with Welch's correction was used for data represented in Figure D. P value denoted as *<0.05, **<0.01 and ***< 0.001.

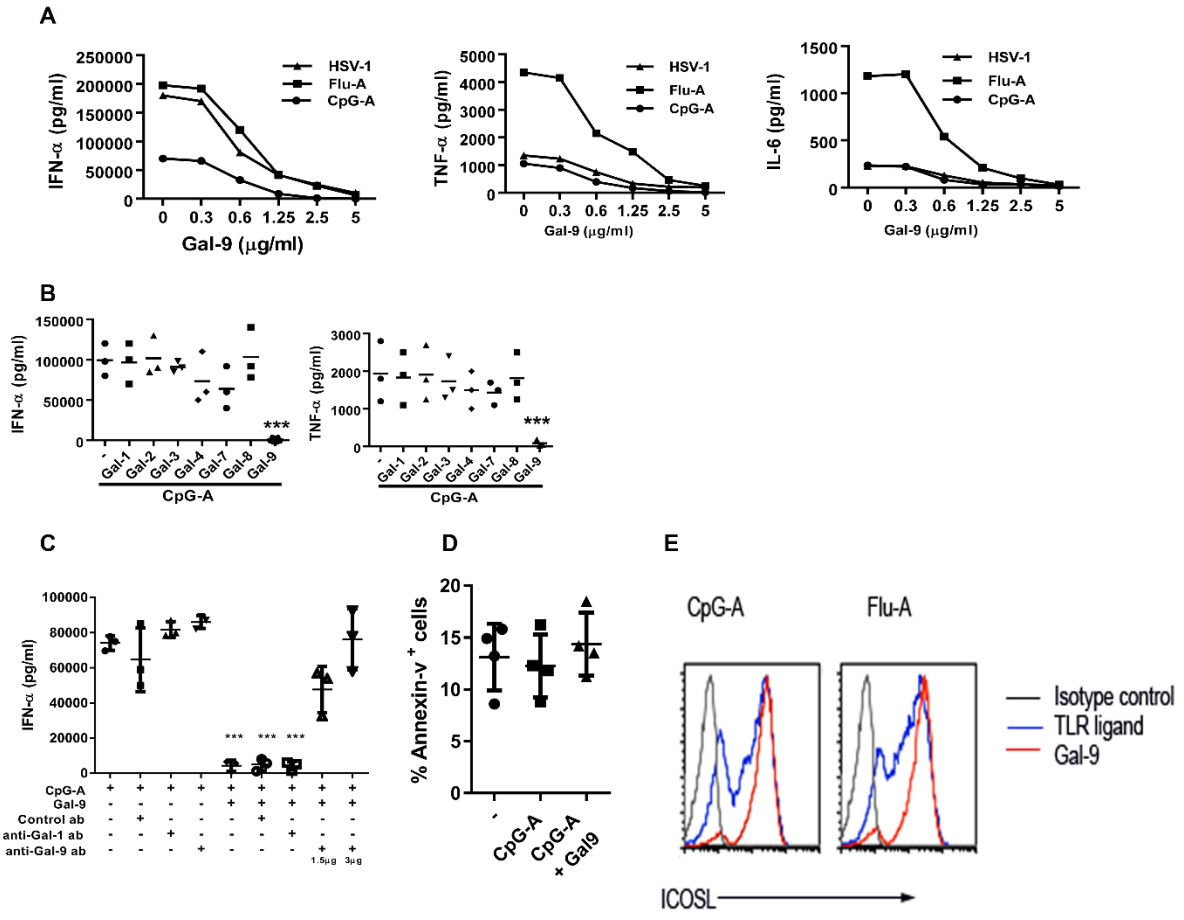

Supplemental Figure 5. Gal-9 inhibits TLR induced pDC activation in a dose dependent manner.

(**A**)Human pDCs were stimulated HSV-1, Flu-A and CpG-A with different doses of Gal-9 for 24 hours and levels of IFN-α, TNF-α and IL-6 were analyzed in the culture supernatant. (**B**)Human primary pDCs from healthy donors were stimulated with CpG-A in the presence or absence of recombinant human galectins 1, 2, 3,4,7,8 and 9. Culture supernatants were analyzed for IFN-α and TNF-α. Data shown are mean of three independent experiments. Human pDCs were stimulated with CpG-A, Gal-9, control antibodies, anti-Gal-1 antibodies and anti-Gal-9 antibodies alone or with different combinations for 24 hrs. The culture supernatants were analyzed for levels

of IFN-α (**C**). Human pDCs were stimulated with CpG-A along with Gal-9 for 24 hrs and the cells were stained using Annexin-V kit and analyzed by FACS (**D**) Human pDCs stimulated with CpG-A and Flu-A and Gal-9 for 24 hours and stained for ICOSL expression by FACS (**E**). Kruskal Wallis testing was performed followed by Dunn's test for statistical analysis. P value denoted as *<0.05, **<0.01 and ***< 0.001.

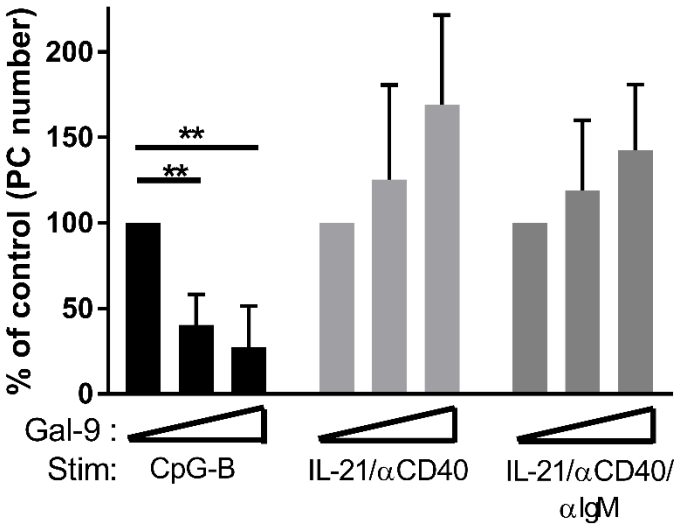

Supplemental Figure 6. Gal-9 specifically inhibits TLR mediated PC differentiation.

Human peripheral B cells were stimulated with CpG-B, anti-CD40 antibodies, anti-IgM, IL-21 and Gal-9 in different combinations as indicated. On day 7 following activation, PCs were quantified by flow cytometry, identified as $CD19^{+/lo}$ $CD27^{high}$ $CD38^{hi}$ cells. The number indicates percent PCs of total $CD19^{+}$ B cell population. Kruskal Wallis testing was performed followed by Dunn's test for statistical analysis. P value denoted as *<0.05, **<0.01.

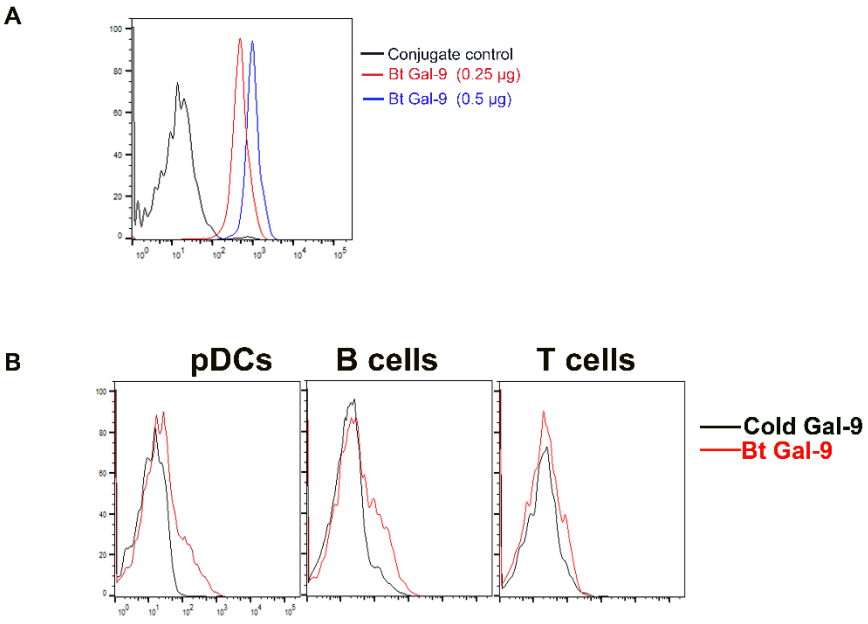

Supplemental Figure 7. Gal-9 binds to the surface of B cells.

(**A**)Human B cells were incubated with different concentrations of biotinylated Gal-9 (Bt Gal-9), probed with streptavidin-APC analyzed by FACS. Overlaid histograms of the binding of Bt Gal-9 to the surface of human B cells. (**B**) Biotin labelled (Bt Gal-9) and unlabeled (Cold Gal-9) were injected to C57/Bl6 mice and after two hrs, different peripheral cells were analyzed to detect the binding of Bt Gal-9 to the surface. Representative overlaid histograms of 3 mice in each group.

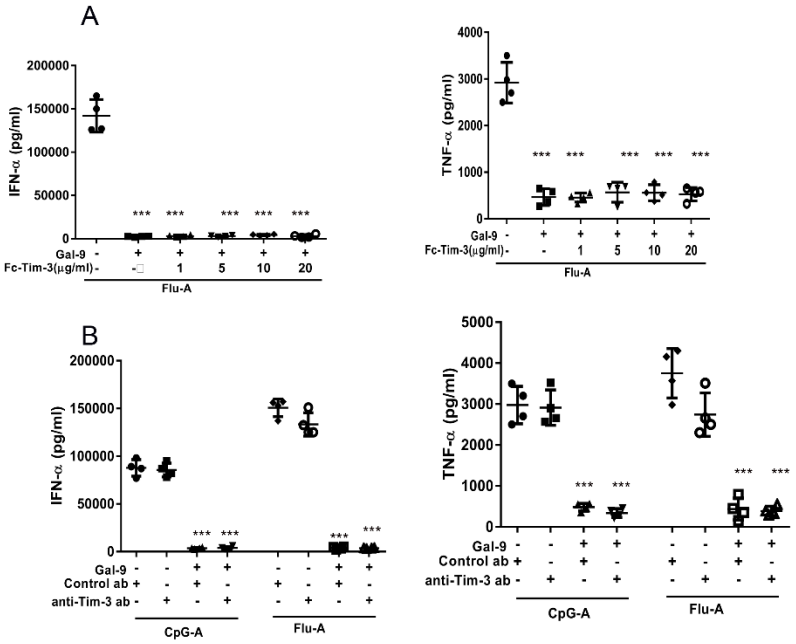

Supplemental Figure 8. Inhibition of TLR induced pDC activation by Gal-9 is independent of Tim-3.

Human pDCs were stimulated with CpG-A, Flu-A, Gal-9, Tim-3 recombinant protein, anti-TIM-3 antibodies and isotype IgG alone or in various combinations for 24 hours. The culture supernatants were analyzed for levels of IFN-α and TNF-α (**A, B**). Data represented is mean±SD of 4 independent experiments. Kruskal Wallis testing was performed followed by Dunn's test for statistical analysis. P value denoted as ***< 0.001.

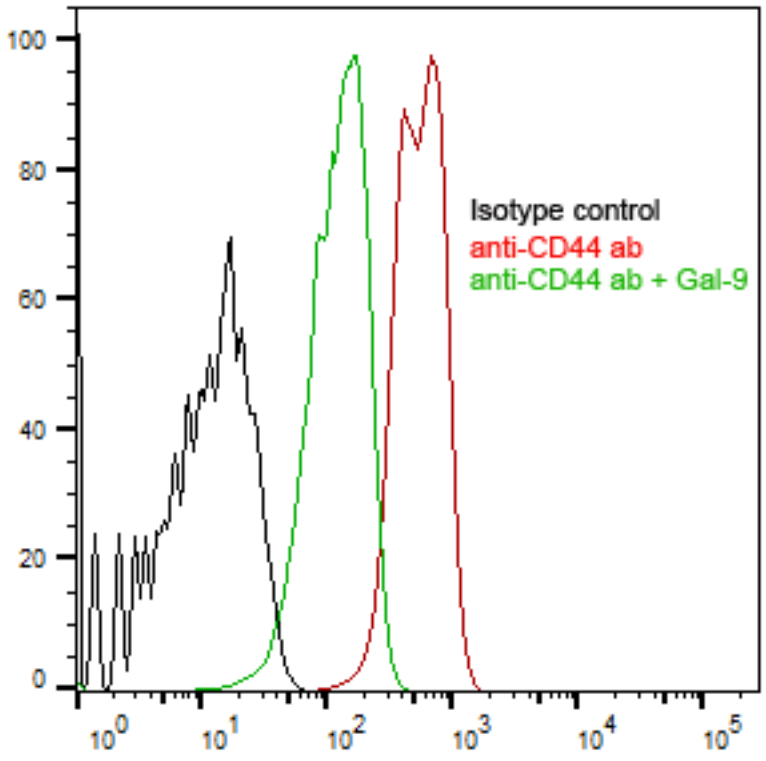

Supplemental Figure 9. Gal-9 inhibits interaction of anti-CD44 antibodies to the surface of human B cells.

Human B cells were incubated with anti-CD44 antibodies with and without Gal-9 and analyzed by FACS. Overlaid histograms of the binding of anti-CD44 antibodies to the surface of human B cells with and without Gal-9. Data representative of five independent experiments.

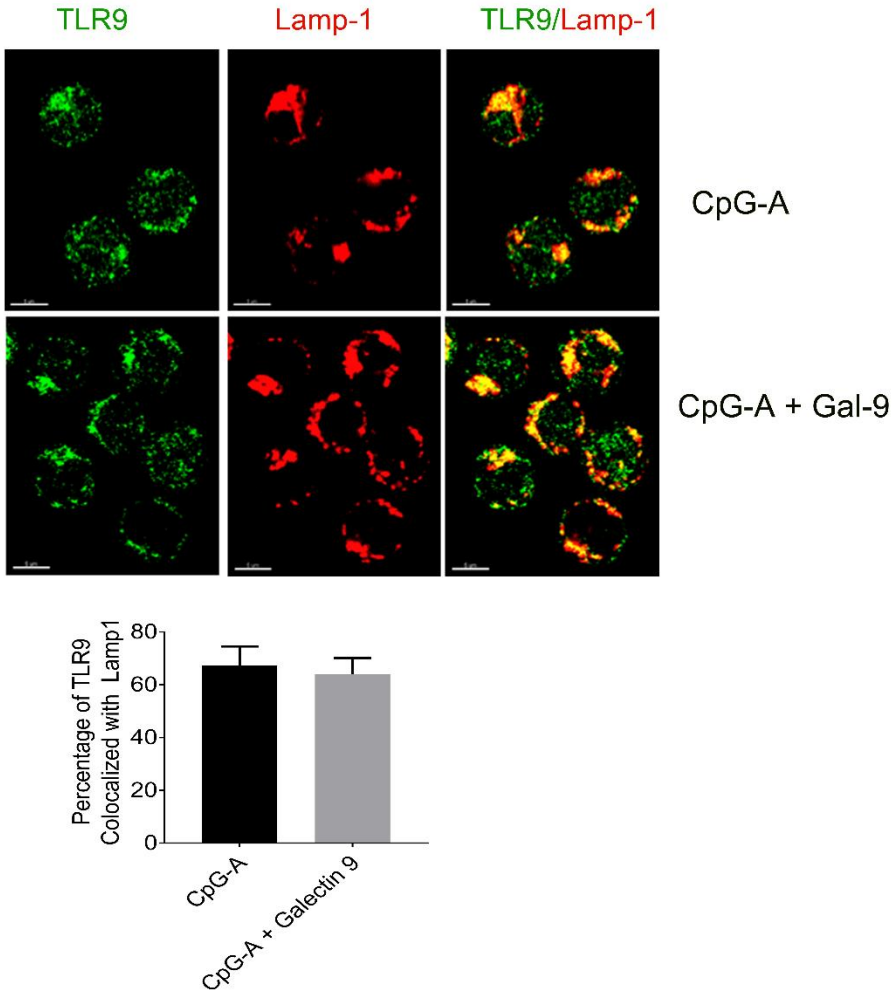

Supplemental Figure 10. Colocalization of TLR9 with the lysosomal marker Lamp1.

Gal-9 treatment did not affect CpG-A induced TLR9 colocalization with the lysosomal marker Lamp1 in primary human pDCs as detected by fluorescent microscopy. After CpG-A treatment in the presence (top panel) or absence (bottom panel) of Gal-9, pDCs were stained with anti-TLR9 antibody labeled in A488 (Green) and anti-Lamp1 antibody labeled in A594 (Red) and then imaged by confocal microscopy . Colocalization of TLR9 and Lamp1 is shown.

Quantification of seven images with multiple cells each from two separate donors. Unpaired student's T test was performed to test the statistical significance.

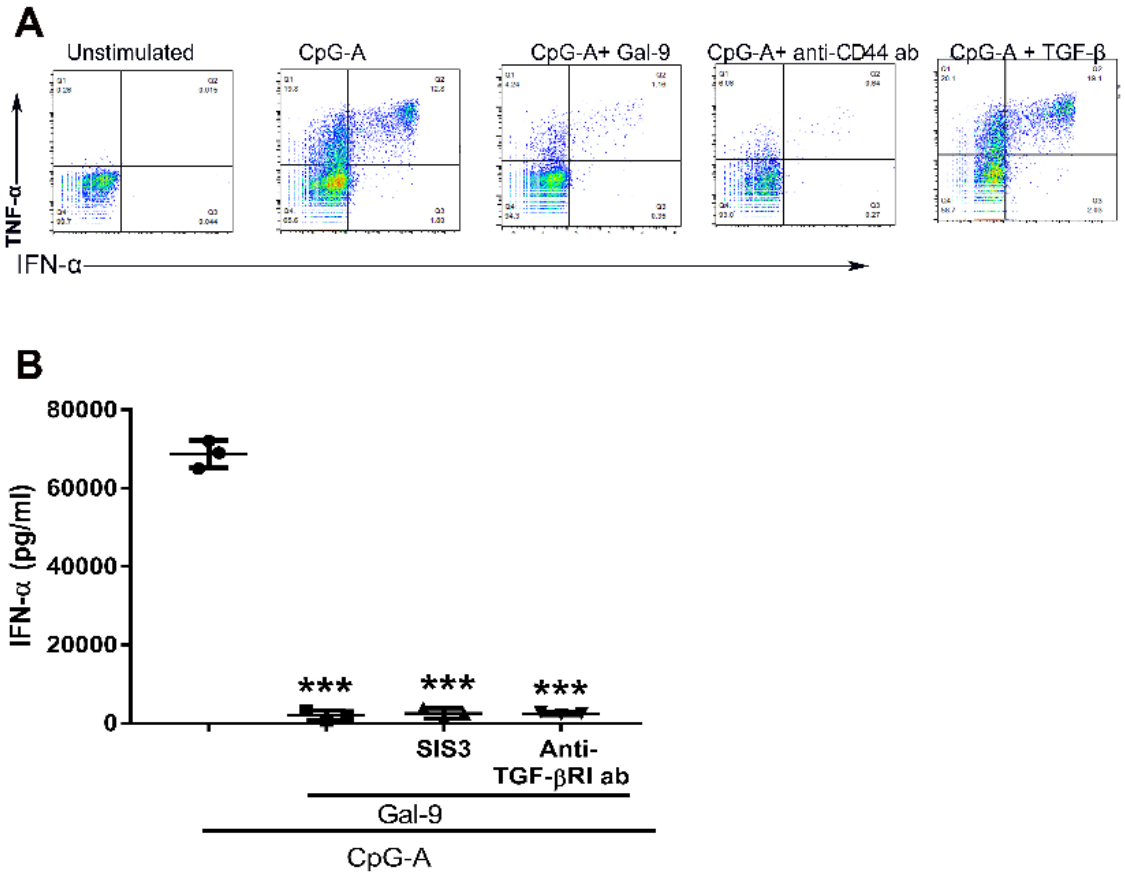

Supplemental Figure 11. Inhibitory effect of Gal-9 is independent of TGF-βRI-Smad-3 pathway.

Human pDCs were stimulated with CpG-A, Gal-9, anti-CD44ab and TGF-β in various combinations for 6 hrs and expression of intracellular TNF-α and IFN-α was analyzed by FACS. Cells in the upper right quadrant were positive for both cytokines (**A**). Human pDCs were stimulated with CpG-A, Gal-9, SIS3 and anti-TGF-βRI antibody in various combinations for 24

hrs and levels of IFN-α in the culture supernatant were analyzed (**B**). Data are representative of three independent donors. Kruskal Wallis testing was performed followed by Dunn's test for statistical analysis. P value denoted as ***< 0.001.

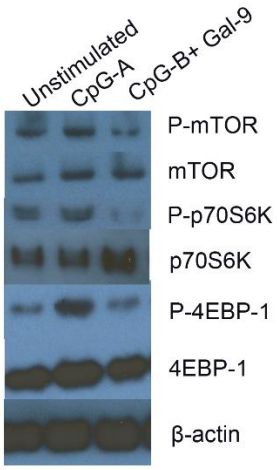

Supplemental Figure 12. Gal-9 inhibits mTOR-p70S6K pathway in human B cells.

Human peripheral B cells were treated with CpG-B with or without Gal-9 for 15 minutes and the cell lysates were analyzed by western blotting. Data are representative three independent experiments.

Supplemental methods

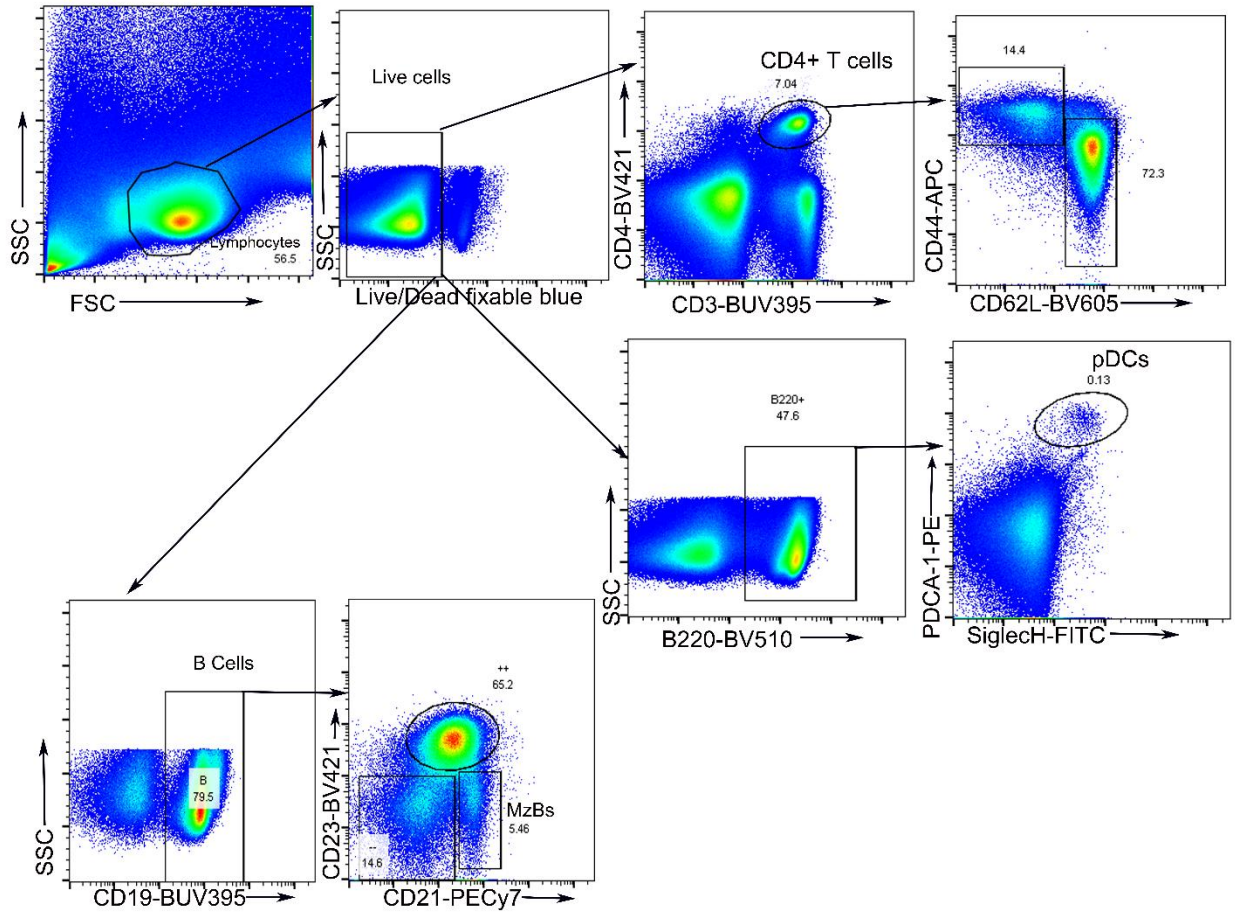

Representative figure showing the gating strategy in flow cytometry.

Lymphocytes were gated in a forward scatter (FSC)/ side scatter (SSC) plot. The dead cells from the lymphocyte population were excluded using live/dead blue stain kit. Live lymphocytes were further analyzed into T cells ($CD3^+$ $CD4^+$), pDCs ($B220^+$, PDCA-1 $^+$and $SiglecH^+$) and B Cells ($CD19^+$). Expression of CD44 and CD62 by T cells and CD21 and CD23 by B cells were analyzed.

Measurement of TLR9 internalization with Galectin 9 treatment

PDCs were incubated with CPG-A with or without the addition of Gal-9 for two hours. Cells were fixed and stained with anti-human Lamp1-A647 (H4A3), anti-human TLR9-A488 (PA-5-46898). Cells were imaged in 96 well glass bottom plates using a Zeiss 880 microscope, and images were analyzed using Imaris imaging software (Bitplane). For analysis of colocalization a similar fluorescent threshold was applied to all images, and percentage of TLR9 fluorescent signal overlapping with Lamp1 fluorescent signal was quantified from 7 images with multiple cells per image.